Mobilization of Pollutant-Degrading Bacteria by Eukaryotic Zoospores

Rungroch Sungthong,[†,‖] Pieter van West,[‡] Fredrik Heyman,[§] Dan Funck Jensen,[§] and Jose Julio Ortega-Calvo*[,†]

[†]Instituto de Recursos Naturales y Agrobiología de Sevilla (IRNAS-CSIC), Apartado 1052, Seville 41080, Spain

[‡]Aberdeen Oomycete Laboratory, University of Aberdeen, Institute of Medical Sciences, Foresterhill, Aberdeen AB25 2ZD, UK

[§]Uppsala BioCenter, Department of Forest Mycology and Plant Pathology, Swedish University of Agricultural Sciences, Uppsala 750 07, Sweden

Running title: Enhancing Bacterial Mobilization by Zoospore Taxis

Word count: 4876 words, 2 figures, 2 tables and 29 references cited.

Keywords: Eukaryotic zoospores; Pollutant-degrading bacteria; Mobilization; Swimming behavior; Bioremediation

ABSTRACT: The controlled mobilization of pollutant-degrading bacteria has been identified as a promising strategy for improving bioremediation performance. We tested the hypothesis whether the mobilization of bacterial degraders may be achieved by the action of eukaryotic zoospores. We evaluated zoospores that are produced by the soil oomycete *Pythium aphanidermatum* as a biological vector, and, respectively, the polycyclic aromatic hydrocarbon (PAH)-degrading bacteria *Mycobacterium gilvum* VM552 and *Pseudomonas putida* G7, acting as representative non-flagellated and flagellated species. The mobilization assay was performed with a chemical-in-capillary method, in which zoospores mobilized bacterial cells only when they were exposed to a zoospore homing inducer (5% (v/v) ethanol), which caused the tactic response and settlement of zoospores. The mobilization was strongly linked to bacterial motility, because the non-flagellated cells from strain *M. gilvum* VM552 and slightly motile, stationary-phase cells from *P. putida* G7 were mobilized effectively, but the actively motile, exponentially-grown cells of *P. putida* G7 were not mobilized. The computer-assisted analysis of cell motility in mixed suspensions showed that the swimming rate was enhanced by zoospores in stationary, but not in exponentially-grown, cells of *P. putida* G7. It is hypothesized that the directional swimming of zoospores caused bacterial mobilization through the thrust force of their flagellar propulsion. Our results suggest that, by mobilizing pollutant-degrading bacteria, zoospores can act as ecological amplifiers for fungal and oomycete mycelial networks in soils, extending their potential in bioremediation scenarios.

TOC ART

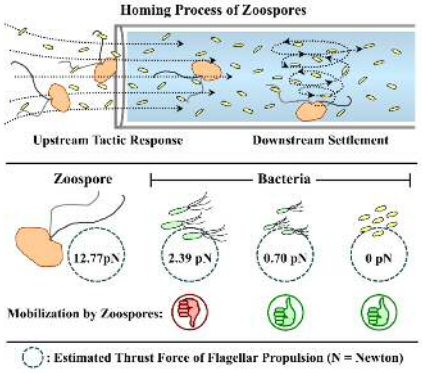
Homing Process of Zoospores
Upstream Tactic Response
Downstream Settlement
Zoospore
Bacteria
12.77pN
2.39 pN
0.70 pN
0 pN
Mobilization by Zoospores:
: Estimated Thrust Force of Flagellar Propulsion (N = Newton)

INTRODUCTION

The microbial communities that are present at the solid-liquid interfaces of polluted environments are often responsible for enhanced rates of pollutant biodegradation, as compared with freely suspended communities.[1] Interface communities usually start after mobilization or translocation of microbial cells to the interface of the pollutant-containing matrices, which may be restricted by the deposition and attachment of cells on adjacent surfaces along their travelling distance.[2,4] Self-propelled pollutant-degrading microbes (e.g., *Pseudomonas* spp.) swim using their flagella, and they access pollutants through chemotaxis, which has been recognized as a biological means for increasing pollutant bioavailability and biodegradation.[1,5] However, pollutant-degrading microbes that lack flagella (e.g., *Mycobacterium* spp.) have other dispersal mechanisms, which may include surface motility and/or gliding movements on moist surfaces.[6] It is unclear how these flagella-independent mechanisms contribute to overcome the restricted bioavailability of pollutants, since these pollutant-degrading microbes have been found to dominate specific microniches in polluted soils, such as those associated to pollutant-enriched clay fractions.[7] In any case, the directional mobilization of pollutant-degrading microbes has been identified as a promising strategy for improving bioremediation performance.[1]

With an aim of improving microbial accessibility during bioremediation, some chemical effectors have been found to modulate the motility behaviors of self-propelled bacteria, leading to enhanced transport through porous media.[3,4] Nonetheless, little is known about the influence of biological effectors on bacterial mobilization, e.g., other microbes that may co-exist with pollutant-degrading bacteria. Some studies have reported mycelial networks of fungi and oomycetes

97 that have the capacity to provide water-saturated routes, facilitating the tactic
98 movement of flagellated polycyclic aromatic hydrocarbon (PAH)-degrading
99 bacteria towards PAHs.[8-10] We recently showed that the zoospores that are
100 produced by the oomycete *Pythium aphanidermatum* can interact synergistically
101 with either flagellated or non-flagellated PAH-degrading bacteria in a set of
102 PAH-polluted microenvironments.[11] In that study, we determined that
103 PAH-degrading bacteria acted positively on zoospore development, for example,
104 by enhancing zoospore taxis to root exudates and diminishing the toxic influence
105 of PAHs on zoospore formation and taxis. Furthermore, the interactions between
106 zoospores and bacteria resulted in the initiation of complex biofilms at
107 pollutant-water interfaces. The enhancement of PAH bioavailability through
108 microbial colonization at pollutant-water interfaces by zoospore settlement,
109 germination and the formation of mycelial networks was therefore identified.
110 Despite these advancements, little is known about the mechanisms involved in the
111 dispersal of pollutant-degrading bacteria by eukaryotic zoospores.

112 For decades, scientists have been trying to understand the fluid mechanics
113 of microbial motion, in both quiescent and flowing regimes.[12-15] The
114 physicochemical properties of fluids are used to interpret hydraulic activities, in
115 which the inertial-to-viscous forces ratio is one of the descriptive parameters in
116 fluid dynamics; this ratio is described by the Reynolds number (*Re*).[12-15] The *Re*
117 value of a macroswimmer (for example a fish swimming in a river) is typically
118 much higher than 1, what correspond to the so-called “high-*Re* environments”.
119 The *Re* of the aqueous microenvironments surrounding microbial cells (an
120 example for a “low *Re* environment”)- is much lower than 1 for a fluid flow with
121 smooth and laminar motion at low velocities and small length scales.[13,15] The

122 unique locomotion of self-propelled microbes within low-*Re* environments is
123 known to depend on their flagellar motors, which can cause dramatic changes in
124 flow. Some self-propelled microbes create thrust forces in front of their bodies
125 during swimming, and these microbes are known as "pullers" (e.g., biflagellate
126 algae). Microbes that create thrust forces behind their bodies are known as
127 "pushers" (e.g., bacteria).[12,14] In bacteria, the thrust forces created by flagellar
128 propulsion ($f_{propulsion}$) are in the range of 0.1 – 1 pN (N = Newton).[16,17] However,
129 the $f_{propulsion}$ values of eukaryotic zoospores and the impact of these forces on the
130 motion and mobilization of bacterial cells have yet to be known. The estimation of
131 these forces in microswimmers may offer an interpretation of the physical
132 interactions in connection with bacterial dispersal. Other mechanisms that may be
133 involved in biomobilization are changes in the fluid viscosity surrounding the
134 microenvironments of swimmers, [18,19] or the direct association with the vector
135 organism.[20] However, swimming interactions in eukaryotic
136 microswimmer-bacteria mixtures within low-*Re* environments and their relevance
137 to the mobilization of bacterial cells have yet to be shown.

138 With the goal of ecological applications for innovative bioremediation
139 strategies, we have examined the possible role of *P. aphanidermatum* zoospores
140 as a biological vector for mobilizing two representative PAH-degrading bacteria
141 (*Pseudomonas putida* G7 and *Mycobacterium gilvum* VM552). Differences in the
142 motility of zoospores and PAH-degrading bacteria were computed and discussed
143 in relation to the mobilization of bacterial cells and the flow regime in the
144 mobilization assay. The effectiveness of the bacterial mobilization that was caused
145 by physical interactions with zoospore taxis was assessed by numerical
146 estimations using motility data.

MATERIALS AND METHODS

Microbial Strains, Cultivation and Preparation. The oomycete *P. aphanidermatum* was used as a source of zoospores. The primary stock was supplied by the Aberdeen Oomycete Laboratory at the University of Aberdeen, UK. The oomycete was grown on diluted V8 (DV8) agar, and zoospore formation was induced according to a protocol that is described elsewhere.[11] With this protocol, 10^4 – 10^5 zoospores mL^{-1} in zoospore-forming solution (sterilized lake water collected from Embalse Torre del Águila, Seville, Spain) were obtained. The zoospore sizes were determined using a phase-contrast Axioskop 2 Carl Zeiss microscope (Jena, Germany) with a 40×/NA0.65 A-plan objective (Carl Zeiss, Germany) and connected to a Sony Exwave HAD color video camera (Sony, Japan) and are given in Table 1.

The multiple PAH-degrader *M. gilvum* VM552 was supplied by D. Springael (Catholic University of Leuven, Belgium), and the naphthalene-degrader *P. putida* G7 was supplied by C.S. Harwood (University of Washington, USA). Both bacterial strains were cultured in mineral salt media supplemented with phenanthrene (Sigma-Aldrich, Germany) for *M. gilvum* VM552[21] or naphthalene (Sigma-Aldrich, Germany) for *P. putida* G7.[3,4] These bacterial cultures were then preserved in 20% (v/v) glycerol at -80°C and used as a primary stock. For the mobilization assays, both bacterial strains were grown in tryptic soy broth (Sigma-Aldrich, Germany) and incubated at 30°C with reciprocal shaking at 150 rpm. *M. gilvum* VM552 cells were collected in the exponential phase (~96 h of incubation). *P. putida* G7 cells were collected in the exponential (~12 h of incubation) and stationary (~96 h of incubation) phases. The initial densities of bacterial cells that were suspended in the sterilized lake water

were adjusted to an optical density ($OD_{600\ nm}$) of 1.5. This OD corresponded to 10^{10} and 10^{8} colony-forming units (CFU) mL^{-1} for *P. putida* G7 and *M. gilvum* VM552, respectively.[11] The cell sizes of bacteria that are approximately 10 times smaller than the zoospores, are shown in Table 1.

Mobilization Assay. A modified chemical-in-capillary method (Supporting information, SI Figure S1A) was used to investigate the bacterial mobilization caused by zoospores.[11] The chemical-in-capillary method is commonly used for assaying the positive chemotaxis of self-propelled microbes. The level of chemo-attraction performed by the microbes is determined by the difference in viable counts detected in the capillary tubes that are filled with the test solution, and subsequently connected to a chamber filled with the microbial suspension. In this study, we adapted that method by using 5% (v/v) ethanol in the capillaries as an inducer for zoospore homing, that is a set of sequential behaviors, comprised of upstream swimming towards the inducer and downstream settlement (involving the release of flagella and encystment).[11, 22] Microbial suspensions were prepared either with individual suspensions of bacterial cells or with pairwise mixtures of both microbes. The bacterial cell suspensions were prepared by making a 10-fold dilution relative to the initial density ($OD_{600\ nm}$ = 1.5) using sterilized lake water, and the mixtures were prepared by diluting the zoospore suspensions. The final density of zoospores in these experiments was 10^{4} – 10^{5} zoospores mL^{-1}, and the densities of the bacterial cells were 10^{9} and 10^{7} CFU mL^{-1} for *P. putida* G7 and *M. gilvum* VM552, respectively. We estimated from the literature and own experiments[11] that these cell densities would be realistic to use for simulating a natural situation. There was observed no antagonism between the zoospores and bacteria at these cell densities.[11] The formation of oxygen gradients would have

interfered, as a consequence of aerotaxis, with the measurements. However, this can be excluded because the low concentration of dissolved organic carbon in the solutions (9 mg L^{-1})[11] minimized the consumption of oxygen in the chamber. Furthermore, we did not observe any microbial accumulation at the air-liquid interfaces along the edge of the chamber, what would have unequivocally indicated an aerotaxis reaction. The prepared microbial suspension (~500 μL) was introduced to a chamber (depth = 1.09 mm, Figure S1A), where the open-ended 1-μL capillary tubes (inner diameter = 0.20 mm, Microcaps, Drummond, Broomall, PA, USA) filled with the zoospore homing inducer [11, 22] or sterilized lake water (as a control) were inserted. Steady flow through the capillaries allowed zoospore motility and settlement inside the capillaries. The inducer was prepared by diluting absolute ethanol (Panreac, Barcelona, Spain) with sterilized lake water, and the concentration (5% v/v) was chosen on the basis of the distance of zoospore travel into the capillary tubes (SI Figure S1B) and the lack of influence of this concentration on the bacterial cell viability (SI Figure S2A). The chambers were incubated at 25°C for ~1 h. The homing process of the zoospores was determined by recording the numbers of zoospore cysts inside the capillary tubes. The capillary tubes were then taken out of the chamber, and their outer walls were cleaned three times with sterilized distilled water. The whole liquid volume (1 μL) inside each capillary tube was immediatelly transferred with a bulb dispenser into a known volume of sterilized lake water for a serial dilution. The capillary tube-connected dispenser was washed with the dilution solution for at least 3 times to ensure the complete transfer of microbial cells. The number of bacterial cells that entered the capillary tube (CFU μL^{-1}) was quantified after the dilutions were developed on tryptic soy agar (Sigma-Aldrich, Germany)

supplemented with 0.3 g L^{-1} cycloheximide, which prevented oomycete growth. There was no influence on the viability of both bacterial strains from this cycloheximide dose (SI Figure S2B).

Physicochemical Properties and Hydraulic Activities of Fluids in the Mobilization Assay. There were two zones in the mobilization assay, including 1) the chambers that contained microbial cells suspended in sterilized lake water and 2) the connected open-end capillary tubes that contained sterilized lake water or 5% (v/v) ethanol (SI Figure S1A). A steady flow through the tubes occurred as a result of evaporation and capillary forces. In addition, a low concentration of ethanol might have caused changes in the hydrodynamic properties (e.g., fluid density, dynamic viscosity, fluid flow velocity, *Re* and friction force) of the fluid bodies between the two zones. To exclude the possibility that the changes caused by ethanol interfered with the mobilization assay, we estimated the fluid density and dynamic viscosity at the two zones using the Jouyban-Acree model (SI Method S1).[23]

We also measured the hydraulic flow rate (u_0) through the capillary tubes. This value was calculated by determining the linear speed of spontaneously flowing *M. gilvum* VM552 cells, which were used as a microbial tracer, at the mid-depth of capillary tubes filled with 5% (v/v) ethanol. This measurement was performed using the same microscope settings as described above. The focal plane was set to 100 μm below the inner wall of the capillary tube, as the mid-depth of the capillary channel, to minimize the interaction of bacteria with surfaces. Multiple motion records derived from the mobilization experiments were processed with Windows Movie Maker, Microsoft Windows XP. Individual paths were then selected randomly from the motion records and used for motion

247 analysis with the CellTrak program (version 1.5, Motion Analysis Corporation,
248 CA, USA). Ten paths were used for calculations to plot the linear speeds as a
249 function of the recording time. The u_0 value was calculated by linear regression.
250 We assumed that the u_0 values detected at the mid-depth of the capillary tube
251 corresponded to the maximum velocity of the fluid flow (u_{max}) along the capillary
252 channel in accordance to the parabolic velocity profile of the Poiseuille's law.

253 The Reynolds number (*Re*) was calculated using the equation

254 $$Re = \frac{\rho \cdot u_0 \cdot D_H}{\eta} \qquad (1)$$

255 where u_0 is the hydraulic flow rate (in m s^{-1}), ρ is the fluid density in kg m^{-3}, η is
256 the dynamic viscosity of the fluid in Pa s, and D_H is the inner diameter of the
257 capillary tube in m (0.20×10^{-3} m).

258 Two friction forces, including the drag force of fluid motion (F_{drag}) and the
259 thrust force of flagellar propulsion ($f_{propulsion}$) performed by each self-propelled
260 microbe, were estimated in this study. Stokes' law was employed to estimate the
261 value of F_{drag} that acted at the interface between a small spherical particle and a
262 fluid. We assumed here that all microbial cells were nearly spherical particles.
263 Hence, the F_{drag} in Newton (N) of the aqueous microenvironments that affected a
264 single *M. gilvum* VM552 cell was estimated using the following equation:

265 $$F_{drag} = 6 \cdot \pi \cdot \eta \cdot R \cdot u_0 \qquad (2)$$

266 where *R* is the radius of the spherical particles in m (assumed here to be half of
267 the L/B ratio of *M. gilvum* VM552 in Table 1), and the other variables are
268 described above. In low *Re*-environments, $f_{propulsion}$ can be described in the same
269 way of F_{drag}.[16] Therefore, $f_{propultion}$ of each self-propelled microbe was estimated
270 with Equation (2), where *R* was set as the half value of the cell length (Table 1),

271 and u_0 was the swimming speed of the microbe.

272 **Biomobilization Efficiency.** The mobilization efficiency of bacterial cells
273 by zoospores was estimated using the mobilization rate (M_{rate}) and the apparent
274 flow rate (u_Z). The M_{rate} value (in cells μL^{-1} s^{-1} per zoospore) was calculated as

275 $$M_{rate} = \frac{CFU_Z - CFU_0}{(N_Z - N_0) \cdot t} \qquad (3)$$

276 where CFU_Z is the bacterial biomass (CFU μL^{-1}) that was mobilized in the
277 presence of zoospores and their homing inducer, CFU_0 is the bacterial biomass
278 (CFU μL^{-1}) mobilized at u_0, N_Z and N_0 are the numbers of zoospore cysts formed
279 in the capillary tubes that contained the inducer and the sterilized water,
280 respectively, and t is the incubation time in s (~3,600 s). Assuming that the
281 increased bacterial cell concentration in the capillary from the mobilization caused
282 by zoospores was accompanied by enhanced flow, the value of u_Z (in μm s^{-1}) was
283 calculated from the relative fraction of mobilized bacterial cells and the hydraulic
284 flow rate as follows:

285 $$u_Z = u_0 \cdot \left[\frac{CFU_Z}{CFU_0} \right] \qquad (4)$$

286 **Motion Analysis.** The same microbial suspensions that were used for the
287 mobilization assay were used for motion analysis. These determinations included
288 the swimming trajectory, speed, and rate of change of direction (RCDI). Only
289 flagellated microbes were included in the motion analysis. We first observed and
290 recorded the swimming behaviors of flagellated microbes using a phase-contrast
291 microscope connected to a video camera, described above. The focal plane was
292 also set to 100 μm below the inner wall of the capillary tube. Second, multiple
293 motion records derived from either the individual suspensions or the mixtures
294 were processed by cutting the records into 6 s-long segments. The longest

swimming paths were then selected randomly from the motion records and used for motion analysis with the CellTrak program. Four swimming patterns were assigned in this study: linear, circular, sine wave and tortuous. Example for these patterns are shown in SI Figure S3. The swimming speed ($\mu m\ s^{-1}$) and RCDI (deg s^{-1}) were computed under two-dimensional analyses, although upwards swimming action of zoospores was often observed at a rate <1 s^{-1} (data not shown). Both the speed and RCDI were normalized using the average values that were derived from the individual swimming paths and reported as the global speed and global RCDI, respectively.

Statistical Analysis. The mean value ± standard deviation (SD) or standard error (SE) derived from any measurements were reported with the corresponding observation number. A comparison of multiple means was performed by one-way analysis of variance (ANOVA) with Tukey's *post hoc* test in SPSS 16.0 (SPSS, Chicago IL, USA). The statistical results were described and reported with *F*-distributions, degrees of freedom and significant (*P*) values.

RESULTS

Bacterial Mobilization by Eukaryotic Zoospores. Zoospores mobilized *M. gilvum* VM552 cells only in the presence of the zoospore homing inducer (Figure 1A), as indicated by the significant difference in the number of bacterial cells entering the capillary tubes ($F_{(3, 10)} = 37.492$, $P < 0.0005$). A similar result was observed in stationary-phase *P. putida* G7 cells ($F_{(3, 10)} = 139.456$, $P < 0.0005$) (Figure 1E) but not with exponential-phase cells ($F_{(3, 16)} = 2.210$, $P = 0.127$) (Figure 1C). Along with these observations, the homing responses of zoospores to their inducer were confirmed by the significantly higher number of zoospore cysts

that were formed in the capillary tubes ($F_{(5, 17)} = 34.861$, $P < 0.0005$) (Figure 1B, D and F). A set of control experiments showed no evidence for a tactic response (both positive or negative) by *P. putida* G7 cells to the zoospore homing inducer and zoospore cysts (SI Figure S5).

With the aim of discriminating the physicochemical and hydraulic influences of the fluid bodies from the bacterial mobilization caused by zoospores, we calculated the experimental hydraulic flow rate, using the non-flagellated *M. gilvum* VM552 cells as microbial tracers (Figure 2 and SI Video S1; The SI video files can be downloaded from the following link: http://digital.csic.es/handle/10261/96015). The individual motion speeds were plotted against the measurement times, and the resulting regression equation had a slope close to 0, thus indicating a steady flow ($\partial u_0/\partial t \approx 0$) in addition to a flow rate of 19.51 μm s^{-1}. Although these estimations were performed with ethanol-containing capillaries, the flow rate was assumed to be the same in the ethanol-free controls. This assumption was supported by the absence of significant differences in the number of *M. gilvum* VM552 cells that were mobilized in the absence of zoospores (Figure 1A, Control). The negligible influence of ethanol on the hydrodynamic properties of the solutions that were introduced into the capillaries was also confirmed by calculating their fluid density, dynamic viscosity, Re, F_{drag} and $f_{\text{propulsion}}$ (SI Table S1). For example, Re remained at very similar values with and without ethanol, i.e., 4.4×10^{-3} and 3.7×10^{-3}, respectively.

Using the numerical data derived from the mobilization assay (Figure 1), we estimated the efficiency of bacterial mobilization caused by zoospore taxis by determining the mobilization rate (M_{rate}) and the apparent flow rate (u_Z) in the

experiments with *M. gilvum* VM552 and stationary-phase *P. putida* G7 cells. The results for the *P. putida* G7 cells in exponential phase were not included in these calculations because no significant differences were found between their CFU_Z and CFU_0 values. The M_{rate} values were very similar for the two bacterial species (24 cells μL^{-1} s^{-1} per zoospore for *P. putida* G7 and 22 cells μL^{-1} s^{-1} per zoospore for *M. gilvum* VM552). These mobilization activities led to u_Z values of 45.36 μm s^{-1} for *M. gilvum* VM552 and 87.88 μm s^{-1} for stationary-phase *P. putida* G7 cells, which were two- and four-fold higher, respectively, than the hydraulic flow rate (19.51 μm s^{-1}). The differences in u_Z values between the two species, having a similar cell size (Table 1), suggest different hydrodynamic properties of stationary-phase *P. putida* G7 cells possessing immotile or slightly active flagella.

Swimming Behaviors and Physical Interactions in Microbial Suspensions. Given the significant differences in size and motility between zoospores and bacterial cells (Table 1), the swimming capabilities and interactions between both microbes might explain the mobilization activities observed in this study. In fact, both the bacteria and zoospores exhibited significant changes in their swimming behaviors in the mixed suspensions (Table 2). Randomly selected swimming trajectories of *P. putida* G7 cells and zoospores are displayed in SI Figures S6 and S7, respectively. In the absence of zoospores, exponential- and stationary-phase *P. putida* G7 cells showed dissimilar swimming behaviors. The stationary-phase cells swam at significantly lower speeds and higher RCDI than did the exponential-phase cells. The tortuous movement of both bacterial cell types increased significantly in the presence of zoospores, but the global swimming speed increased significantly only for stationary-phase cells. As a result, the value of $f_{propulsion}$ also increased. The global speed of stationary-phase *P.*

putida G7 cells remained at a significantly lower value than that of the zoospores (approximately 80 μm s^{-1}). However, when scaled to body lengths (Table 1), global speeds of bacteria were significantly higher. The exponential-phase *P. putida* G7 cells impacted the swimming behaviors of zoospores to a greater extent than did the other bacterial cells, as evidenced by the significant decreases in global speed and RCDI. The relative differences between the $f_{propulsion}$ values for zoospore and bacterial swimming were the highest with stationary-phase *P. putida* G7 cells. No significant attachment of bacterial cells to zoospores was observed in any mixed suspension.

These observations were related to the separated suspensions, which were not exposed to any ethanol gradient. These findings would represent the motility interactions that occurred in the primary chamber of the mobilization assay. A set of motion records derived directly from the mobilization assay revealed a clear pattern in the enhancement of bacterial mobilization by the homing responses of the zoospores, which either swam inside the capillary tubes or engaged in encystment, releasing their flagella (SI Video S2 and Figure S4). Circular motion was a key swimming pattern that was often performed by zoospores prior to their encystment (SI Video S3). In addition, swimming *P. putida* G7 cells were found either inside or outside the capillary tubes (SI Video S4), showing the negligible influence of the inducer on bacterial motility. This finding was in accordance with the control experiments (Figure S5), with no effect on the CFU counts in the capillaries.

DISCUSSION

We found that swimming zoospores caused the directional mobilization of

PAH-degrading bacteria. This only occurred in the presence of the zoospore homing inducer. The response of zoospores to their inducer is initiated by swimming towards the chemical gradient of the inducer, followed by settlement on solid-liquid and air-liquid interfaces.[11,22,24] In fact, the cumulative settlement (so called auto-aggregation) of oomycete zoospores can occur through a combination of chemotaxis and bioconvection mechanisms.[25] The bacterial mobilization that was observed in our study resembles the mobilization or transport of microscale loads that result from the tactic responses to light of *C. reinhardtii*.[20] That study showed that *C. reinhardtii* cells swam by phototaxis at speeds of ~100 – 200 μm s^{-1} and transported attached microbeads for a maximum distance of 20 cm. However, in our study we did not observe any significant attachment of bacterial cells to zoospores, which indicates that the mobilization occurred through a different mechanism.

Our results indicate that mobilization by zoospores was strongly linked to a lack of bacterial motility. This finding suggests a mobilization mechanism related to flow dynamics. Slightly motile and non-flagellated bacterial cells were mobilized effectively by zoospores, but the actively motile cells were not mobilized. In mono-specific suspensions and in zoospore and bacteria mixtures, the observed bacterial swimming behaviors were consistent with the mobilization assay results. The exponential-phase *P. putida* G7 cells swam actively, at a global speed that was very similar to the swimming speed of zoospores (Table 2). This high speed likely made the bacterial motion independent of the changes that were caused in the fluid body by the swimming zoospores, because the global speeds of the bacterial cells did not change in the mixed suspensions (Table 2). However, the stationary-phase *P. putida* G7 cells swam at a slower speed, which increased

significantly in the presence of zoospores. This change may be related to the mobilization observed in Figure 1, if we postulate that the slow bacterial motion increased the susceptibility to zoospore mobilization. This finding would also apply to the non-flagellated *M. gilvum* cells. An increased global speed would facilitate dispersion, as observed previously with *P. putida* G7 cells that were exposed to glucose.[4] In that study, glucose consumption and overflow energy dissipation resulted in hypermotility behavior and increased dispersion in capillary assays, compared with those for the glucose-free controls.

The precise biophysical mechanism by which zoospores mobilized the bacterial cells is unknown. However, the distribution and transport of bacterial cells are often affected by the physicochemical properties and hydraulic activities of the surrounding fluids, [3,4,14] that may have changed as a result of zoospore homing. The capillary force, liquid volatility and air pressures might reflect the flow regime in our experimental system. On the basis of calculations with the relevant physical parameters of the ethanol solutions and the results from the mobilization experiments without zoospores, we excluded the possibility that the presence of ethanol in the capillaries interfered physically in the mobilization assays. Based on the estimated flow regime in the mobilization assay, the *Re* values of the solutions present in the capillaries were much lower than 1, which is characteristic of microswimmers.[13] The values calculated here were of the same order for single swimming cells, at 10^{-4}.[15] Under these conditions, and considering the relative differences in the cellular dimensions, swimming speeds and $f_{\text{propulsion}}$ of all microbes used (Table 2 and SI Table S1), the results can be explained by postulating that the thrust force created during zoospore swimming mobilized the bacterial cells. Indeed, swimming zoospores possessed the greatest $f_{\text{propulsion}}$, which

445 was, respectively, 50- and 20-fold higher than the inherent drag force of the
446 flowing fluids and $f_{propulsion}$ in stationary-phase *P. putida* G7 cells. However, some
447 self-propelled bacteria and algae can change the viscosity of their surrounding
448 liquids, and these changes are dependent on their cell density and swimming
449 mechanisms, occurring mainly a high cell densities (i.e., > 10^{10} bacteria/mL).[18,19]
450 Mobilization may have also been associated, in some extent, to viscosity changes
451 caused by the directional swimming of zoospores. It is also possible that the
452 unique swimming behaviors of zoospores that were observed here as a result of
453 their tactic responses and prior to their encystment and settlement could have
454 provided pathways for bacterial mobilization through jet-like fluid motion.[15] For
455 example, the circular motion of zoospores could have acted as a microscale
456 vortexing mechanism. This phenomenon should be investigated further.

457 Our results show that zoospores can act as ecological amplifiers of fungal
458 and oomycete actions, and they can extend, in several aspects, the concept of
459 "mycelial pathways" for PAH-degrading bacteria.[8-10] First, because those studies
460 were performed, possibly to highlight the role of mycelia in transport, with an
461 oomycete (*Pythium ultimum*), that is not normally producing zoospores. Second,
462 the mobilization observed may be of relevance for non-flagellated bacterial PAH
463 degraders, such as *Mycobacterium* species, which may constitute a significant
464 fraction of the functional microbiome in PAH-polluted environments.[6,7] Although
465 they seem to be less well transported through mycelial pathways than
466 self-propelled bacteria,[9] in our study the absence of motility was, in relative terms,
467 a positive factor for the biomobilization caused by zoospores. Finally, flagellated
468 (and therefore chemotactically active) bacterial groups, such as *Pseudomonas* and
469 *Achromobacter*, can be dispersed through their own chemotactic navigation along

mycelial pathways,[8] but they could also be biomobilized by zoospores at the cell growth phases when flagellar motility is limited or not existing.

It is at present unclear as to whether eukaryotic zoospores play a significant role in biomobilization processes under natural conditions in polluted soils. Oomycetes including species of *Pythium* and the closely related *Phytophthora* are found in most soils and often in close association with organic material and plant surfaces. Some are plant pathogenic, causing important plant diseases (damping-off of seedlings, root rot etc.) or they can function in biocontrol interactions. However, methods used in studying filamentous fungi from plant or soil samples are normally not designed for detecting oomycetes – traditional methods as dilution plating will mainly detect conidia-forming fungi and if special selective media and procedures are not used will not reveal oomycetes. Next generation sequencing methods are likewise biased, as they normally have been focussing on the internal transcribed spacer region for determining fungal community structures and the choice/design of primers is crucial for what organisms will be revealed. Barcoding of *Pythium* species would require special attention.[26] Both methods will normally reveal presence of organisms in terms of species richness but not function and will not give information of the stage the organism is present in (mycelium, conidia, resting structure, zoospores, etc.). Possibly for these reasons, very little is known about what relative roles fungi and oomycetes play in polluted areas. The closely related oomycete *Saprolegnia delica* has, however, been repeatedly isolated from drainage water polluted with heavy metals and it was shown to be involved in bioaccumulation of heavy metals.[27] Other studies also report the presence of oomycetes in sites polluted by heavy metals[28] and hydrocarbons.[29] Based on the knowledge from natural

ecosystems and managed soil systems, oomycetes are indeed having important ecological functions and we believe this is the case also in biofilms in polluted soils. Thus, we argue that the role of oomycetes may be overseen in studies of eukaryotes in biofilm formation either due to methodological bias or because they were not considered. The role of zoospores released from true fungi in bioremediation might also be relevant to address in future research as they will have different swimming behaviours, as compared to *Pythium* zoospores.

Our findings would suggest that the active production of motile propagules from mycelial networks, with specific sensing mechanisms related to taxis and settlement, should be considered when designing new inoculants composed of soil fungi and oomycetes and pollutant-degrading bacteria, aimed at the improvement of bacterial accessibility during bioremediation.

ASSOCIATED CONTENT

Supporting Information

(Method S1) Estimating fluid density and dynamic viscosity in the mobilization assay; (Table S1) physicochemical properties and hydraulic activities of fluids in the mobilization assay; (Figure S1) chemical-in-capillary method; (Figure S2) bacterial growth in the presence of 5% (v/v) ethanol or cycloheximide; (Figure S3) determination of swimming patterns in self-propelled microbes; (Figure S4) effects of circular zoospore motion on bacterial mobilization; (Figure S5) control experiment for tactic responses of *P. putida* G7 cells in exponential phase to zoospore cysts and inducer; (Figure S6) swimming trajectories of zoospores; (Figure S7) swimming trajectories of *P. putida* G7 cells; (Video S1) determination of the flow velocity for a fluid body; (Video S2) mobilization of bacterial cells by

zoospore taxis; (Video S3) circular motion and settlement of zoospores; (Video S4) freely swimming *P. putida* G7 cells during the mobilization assay.

AUTHOR INFORMATION

Corresponding Author

*Phone: (+34) 954 624 711; Fax: (+34) 954 624 002;

E-mail: jjortega@irnase.csic.es

Present Address

‖Infrastructure and Environmental Research Division, School of Engineering, University of Glasgow, Glasgow G12 8LT, UK

Notes

The authors declare no competing financial interest.

ACKNOWLEDGMENTS

This study was supported by the Spanish Ministry of Science and Innovation (CGL2010-22068-C02-01 and CGL2013-44554-R), the Andalusian Government (RNM 2337), and the CSIC JAE Program (RS). PvW has funding support from the BBSRC and NERC. Thanks are also given to Sara Hosseini of the Uppsala BioCenter, SLU, Uppsala, Sweden for a useful discussion on oomycete zoospores.

REFERENCES

(1) Krell, T.; Lacal, J. S.; Reyes-Darias, J. A.; Jimenez-Sanchez, C.; Sungthong, R.; Ortega-Calvo, J. J. Bioavailability of pollutants and chemotaxis. *Curr. Opin. Biotechnol.* **2013**, *24*, 451-456.

(2) Hwang, G.; Ban, Y. -M.; Lee, C. -H.; Chung, C. -H.; Ahn, I. -S. Adhesion of *Pseudomonas putida* NCIB 9816-4 to a naphthalene-contaminated soil. *Colloids Surf. B* **2008**, *62*, 91-96.

(3) Jimenez-Sanchez, C.; Wick, L. Y.; Cantos, M.; Ortega-Calvo, J. J. Impact of dissolved organic matter on bacterial tactic motility, attachment, and transport. *Environ. Sci. Technol.* **2015**, *49*, 4498-4505.

(4) Jimenez-Sanchez, C.; Wick, L. Y.; Ortega-Calvo, J. J. Chemical effectors cause different motile behavior and deposition of bacteria in porous media. *Environ. Sci. Technol.* **2012**, *46*, 6790-6797.

(5) Pandey, G.; Jain, R. K. Bacterial chemotaxis toward environmental pollutants: role in bioremediation. *Appl. Environ. Microbiol.* **2002**, *68*, 5789-5795.

(6) Fredslund, L.; Sniegowski, K.; Wick, L. Y.; Jacobsen, C. S.; De Mot, R.; Springael, D. Surface motility of polycyclic aromatic hydrocarbon (PAH)-degrading mycobacteria. *Res. Microbiol.* **2008**, *159*, 255-262.

(7) Uyttebroek, M.; Breugelmans, P.; Janssen, M.; Wattiau, P.; Joffe, B.; Karlson, U.; Ortega-Calvo, J. J.; Bastiaens, L.; Ryngaert, A.; Hausner, M.; Springael, D. Distribution of the *Mycobacterium* community and polycyclic aromatic hydrocarbons (PAHs) among different size fractions of a long-term PAH-contaminated soil. *Environ. Microbiol.* **2006**, *8*, 36-847.

(8) Furuno, S.; Päzolt, K.; Rabe, C.; Neu, T. R.; Harms, H.; Wick, L. Y. Fungal mycelia allow chemotactic dispersal of polycyclic aromatic hydrocarbon-degrading bacteria in water-unsaturated systems. *Environ. Microbiol.* **2010**, *12*, 1391-1398.

570 (9) Kohlmeier, S.; Smits, T. H. M.; Ford, R. M.; Keel, C.; Harms, H.; Wick, L.
571 Y. Taking the fungal highway: mobilization of pollutant-degrading bacteria
572 by fungi. *Environ. Sci. Technol.* **2005**, *39*, 4640-4646.
573 (10) Wick, L. Y.; Remer, R.; Würz, B.; Reichenbach, J.; Braun, S.; Schäfer, F.;
574 Harms, H. Effect of fungal hyphae on the access of bacteria to phenanthrene
575 in soil. *Environ. Sci. Technol.* **2007**, *41*, 500-505.
576 (11) Sungthong, R.; van West, P.; Cantos, M.; Ortega-Calvo, J. J. Development
577 of eukaryotic zoospores within polycyclic aromatic hydrocarbon
578 (PAH)-polluted environments: A set of behaviors that are relevant for
579 bioremediation. *Sci. Total Environ.* **2015**, *511*, 767-776.
580 (12) Koch, D. L.; Subramanian, G. Collective hydrodynamics of swimming
581 microorganisms: Living fluids. *Ann. Rev. Fluid Mech.* **2011**, *43*, 637-659.
582 (13) Purcell, E.M. Life at low Reynolds number. *Am. J. Phys.* **1977**, *45*, 3-11.
583 (14) Rusconi, R.; Stocker, R. Microbes in flow. *Curr. Opin. Microbiol.* **2015**, *25*,
584 1-8.
585 (15) Wolgemuth, C. W. Collective swimming and the dynamics of bacterial
586 turbulence. *Biophys. J.* **2008**, *95*, 1564-1574.
587 (16) Behkam, B.; Sitti, M. Bacterial flagella-based propulsion and on/off motion
588 control of microscale objects. *Appl. Phys. Lett.* **2007**, *90*, 023902.
589 (17) Berke, A. P.; Turner, L.; Berg, H. C.; Lauga, E. Hydrodynamic attraction of
590 swimming microorganisms by surfaces. *Phys. Rev. Lett.* **2008**, *101*, 038102.
591 (18) McDonnell, A. G.; Gopesh, T. C.; Lo, J.; O'Bryan, M.; Yeo, L. Y.; Friend, J.
592 R.; Prabhakar, R. Motility induced changes in viscosity of suspensions of
593 swimming microbes in extensional flows. *Soft Matter* **2015**, *11*, 4658-4668.
594 (19) Sokolov, A.; Aranson, I. S. Reduction of viscosity in suspension of

595 swimming bacteria. *Phys*. *Rev*. *Lett*. **2009**, *103*, 148101.
596 (20) Weibel, D. B.; Garstecki, P.; Ryan, D.; DiLuzio, W. R.; Mayer, M.; Seto, J.
597 E.; Whitesides, G. M. Microoxen: Microorganisms to move microscale
598 loads. *Proc*. *Natl*. *Acad*. *Sci*. *U*. *S*. *A*. **2005**, *102*, 11963-11967.
599 (21) Tejeda-Agredano, M. C.; Gallego, S.; Niqui-Arroyo, J. L.; Vila, J.; Grifoll,
600 M.; Ortega-Calvo, J. J. Effect of interface fertilization on biodegradation of
601 polycyclic aromatic hydrocarbons present in nonaqueous-phase liquids.
602 *Environ*. *Sci*. *Technol*. **2011**, *45*, 1074-1081.
603 (22) Walker, C. A.; van West, P. Zoospore development in the oomycetes. *Fungal*
604 *Biol*. *Rev*. **2007**, *21*, 10-18.
605 (23) Khattab, I. S.; Bandarkar, F.; Fakhree, M. A. A.; Jouyban, A. Density,
606 viscosity, and surface tension of water+ethanol mixtures from 293 to 323K.
607 *Korean J*. *Chem*. *Eng*. **2012**, *29*, 812-817.
608 (24) Appiah, A. A.; van West, P.; Osborne, M. C.; Gow, N. A. R. Potassium
609 homeostasis influences the locomotion and encystment of zoospores of plant
610 pathogenic oomycetes. *Fungal Genet*. *Biol*. **2005**, *42*, 213-223.
611 (25) Savory, A. I.; Grenville-Briggs, L. J.; Wawra, S.; van West, P.; Davidson, F.
612 A. Auto-aggregation in zoospores of *Phytophthora infestan*s: the
613 cooperative roles of bioconvection and chemotaxis. *J*. *R*. *Soc*. *Interface*
614 **2014**, *11*, 2140017.
615 (26) Sapkota, R.; Nicolaisen, M. An improved high throughput sequencing
616 method for studying oomycete communities. J. Microbiol. Methods. **2015,**
617 *110*, 33-39.
618 (27) Ali, E. H.; Hashem, M. Removal Efficiency of the Heavy Metals Zn(II),
619 Pb(II) and Cd(II) by *Saprolegnia delica* and *Trichoderma viride* at different

620 pH values and temperature degrees. *Mycobiol.* **2007,** *35*, 135-44.
621 (28) Ali, E.H. Biodiversity of zoosporic fungi in polluted watr drainages across
622 Niles´ Delta region, Lower Egypt. *Acta Mycol.* **2007**, *42*, 99-111.
623 (29) Steciow, M. M.; Eliades, L. A., *A. robusta* sp nov., a new species of *Achlya*
624 (Saprolegniales, Straminipila) from a polluted Argentine channel. *Microbiol.*
625 *Res.* **2002,** *157*, 177-182.
626

627 **Table 1.** Sizes of Microbial Cells Used in This Study[a]

Microbe	Length (μm)	Breadth (μm)	L/B ratio
P. aphanidermatum			
Zoospores (193)	17.78 ± 2.92	12.58 ± 2.35	1.43 ± 0.18
M. gilvum VM552 (51)	1.52 ± 0.46b	1.03 ± 0.11a	1.48 ± 0.45b
P. putida G7			
Exponential growth phase (50)	3.36 ± 0.83a	1.09 ± 0.11a	3.12 ± 0.82a
Stationary growth phase (50)	1.73 ± 0.40b	1.02 ± 0.10a	1.70 ± 0.36b

628 [a]The numbers in parentheses indicate the number of observations. The length (L),
629 breadth (B) and L/B ratio are shown as the means ± SD. Lower-case letters refer
630 to significant differences in the lengths ($F_{(2, 148)} = 144.130$, $P < 0.0005$), breadths
631 ($F_{(2, 148)} = 6.484$, $P = 0.002$) and L/B ratios ($F_{(2, 148)} = 119.221$, $P < 0.0005$) among
632 the bacteria.

633

634

635

636

637

638

639

640

641

642

643

644

645

646

Table 2 Swimming Behaviors and Physical Interactions in Microbial Suspensions

swimming characteristics	*P. putida* G7			
	exponential-phase cells		stationary-phase cells	
	control	+ zoospores	control	+ zoospores
dominant trajectory (%)	circular (40.60) tortuous (37.40)	tortuous (97.60)	linear (49.40) tortuous (35.30)	tortuous (85.30)
global speed (μm s^{-1})	82.81 ± 2.80c	74.54 ± 1.55c	40.82 ± 2.42a	56.37 ± 2.09b
global RCDI (deg s^{-1})	264.39 ± 18.17a	586.41 ± 19.84b	485.71 ± 27.61b	551.49 ± 23.50b
$f_{propulsion}$ (pN)	2.33	2.10	0.59	0.82
no. of observation	91	83	85	75

swimming characteristics	zoospores			
	control	+ *M. gilvum* VM552	+ *P. putida* G7	
			exponential-phase cells	stationary-phase cells
dominant trajectory (%)	tortuous (67.80%)	tortuous (50.85%) circular (47.46%)	tortuous (60.76%)	tortuous (70.37%)
global speed (μm s^{-1})	82.59 ± 2.46b	88.97 ± 2.68b	74.06 ± 2.08a	86.38 ± 1.82b
global RCDI (deg s^{-1})	772.90 ± 41.73d	464.62 ± 34.21b	256.28 ± 12.55a	634.06 ± 33.18c
$f_{propulsion}$ (pN)	12.30	13.25	11.03	12.86
no. of observations	59	59	79	54

The global speeds and global rate of change of directions (RCDIs) are reported as averages: the means ± SE. The propulsion forces ($f_{propulsion}$) were estimated with Equation (2). Lower-case letters refer to the significant differences in global speeds ($F_{(3, 330)} = 68.597$, $P < 0.0005$) or global RCDIs ($F_{(3, 330)} = 43.511$, $P < 0.0005$) of *P. putida* G7 cells and in the global speeds ($F_{(3, 249)} = 9.926$, $P < 0.0005$) or global RCDIs ($F_{(3, 249)} = 60.243$, $P < 0.0005$) of zoospores.

654 **Figure legends**

655

656 **Figure 1.** Mobilization of bacterial cells by eukaryotic zoospores. *Mycobacterium*
657 *gilvum* VM552 cells (A and B) and exponential- (C and D) and stationary-phase cells (E
658 and F) of *Pseudomonas putida* G7 were used. A mobilization assay was performed in
659 either the absence (control) or presence (+zoospores) of swimming zoospores and either
660 in the absence (white bars) or presence (grey bars) of the inducer. The results are the
661 means of at least triplicate experiments, where the error bars represent the SDs.
662 Asterisks refer to significant differences in the means of bacterial (graphs A, C, or E)
663 and zoospore (graphs B, D and F) counts within each experiment.

664

665 **Figure 2.** Determination of the flow regime in the mobilization assay. *Mycobacterium*
666 *gilvum* VM552 cells that were flowing through a capillary tube filled with the zoospore
667 settlement inducer were used to detect the flow velocities (u) of the fluid body by the
668 CellTrak program. A model shows the detected locations of the flowing cells at different
669 time points inside the capillary tube (32 mm length) (A). The flow velocities of the
670 bacterial cells at the mid-depth plane of the capillary channel (32 mm length) were
671 detected at different time points (u_x, t_x, where x is the point of detection). These detected
672 flow velocities corresponded to the maximum flow velocity (u_{max}) in the parabolic
673 velocity profile of the Poiseuille's law. The results were plotted using the averaged
674 mean velocities derived from ten bacterial cells that were detected at the same time, the
675 error bars represent SDs, and the trending line (dash line) refers to the linear regression
676 equation (B).

677

678

Figure 1.

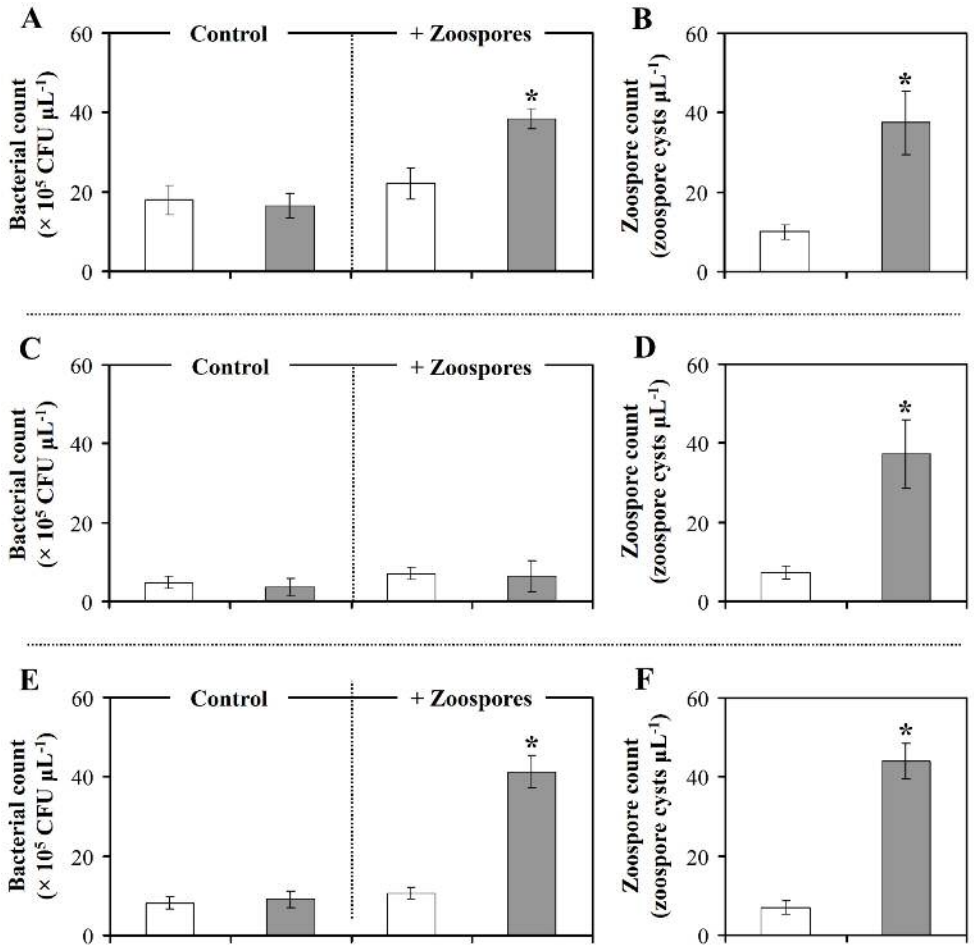
A
Control
+ Zoospores
Bacterial count
(× 10⁵ CFU µL⁻¹)
B
Zoospore count
(zoospore cysts µL⁻¹)
C
D
E
F
0
20
40
60
*

Figure 2.

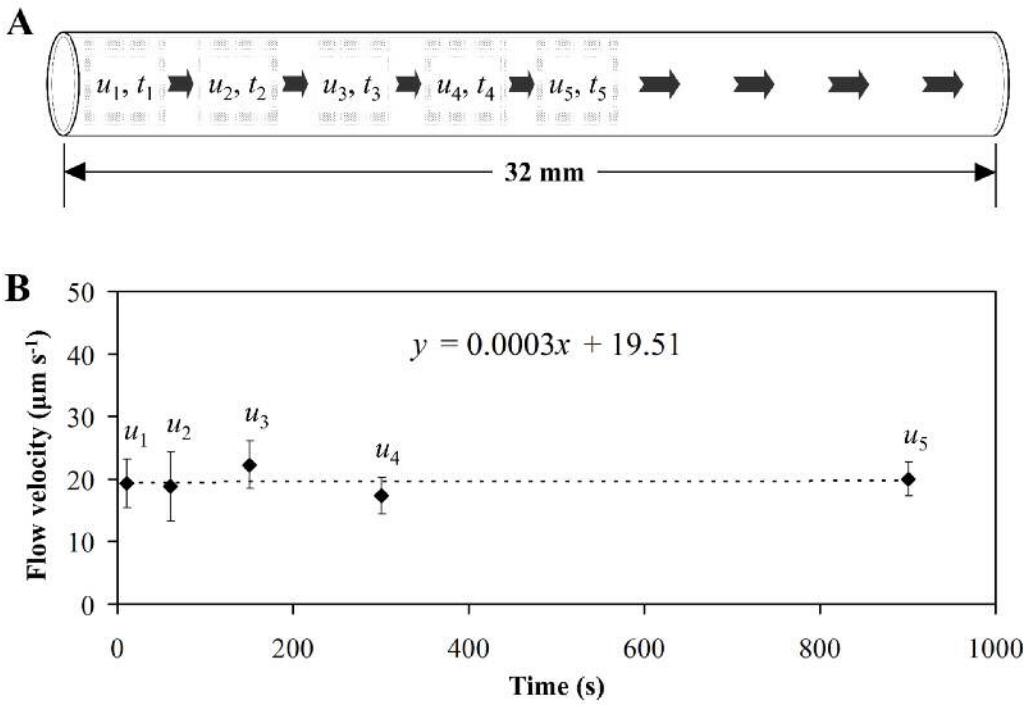
A
u_1, t_1
u_2, t_2
u_3, t_3
u_4, t_4
u_5, t_5
32 mm
B
$y = 0.0003x + 19.51$
Flow velocity (µm s^{-1})
Time (s)
0
10
20
30
40
50
0
200
400
600
800
1000
u_1
u_2
u_3
u_4
u_5